Design and Sustained Release Evaluation of Rifampicin from Polyurethane Membranes

Mihaela Mandru[1,3], Constantin Ciobanu[2], Laurent Lebrun[3], Alexandra Nistor[2], Luiza Madalina Gradinaru[2], Marcel Popa[1] and Stelian Vlad[2,*]

[1]*"Gheorghe Asachi" Technical University, Faculty of Chemical Engineering and Environmental Protection, 71 Dimitrie Mangeron Street, 700050, Iasi, Romania*

[2]*"Petru Poni" Institute of Macromolecular Chemistry, 41A Grigore Ghica Voda Alley, 700487, Iasi, Romania*

[3]*University of Rouen UMR 6270 CNRS, Polymers, Biopolymers, Surfaces, 76821 Mont Saint Aignan Cedex, France*

Abstract: Drug delivery membranes based on polyurethanes have been used for prolonged release of rifampicin. Therefore, two polyurethane structures with concentrations in urethane groups of 1.5 mmol/g and 2.5 mmol/g, respectively were tested for delivery of rifampicin. The influence of the surface morphology in drug release was evaluated by scanning electron microscopy (SEM), atomic force microscopy (AFM) and contact angle measurements. The kinetics, drug release mechanisms and dynamic vapour sorption (DVS) were studied. Prolonged nature of the release of rifampicin is assured by the urethane concentration 2.5 mmol/g but also to the surface of the membrane systems. It was found that the rifampicin release is function of polymer-drug membranes composition and the surface properties. One can assume that the mechanism of diffusion is Fickian, and the experimental data verify this law. Finally, the possibility of applications of the polyurethane matrix with rifampicin was shown by biological test.

Keywords: Biological test, drug delivery, *in vitro*, polyurethane membranes, rifampicin, sustained release.

INTRODUCTION

Many sustained release systems have been developed for the purpose of maintaining a therapeutically effective concentration of drug for a longer period of time, as well as to reduce side effects [1]. The release of drugs depends on how the drug is incorporated into the polymer and on the chemical and morphological properties of the polymers [2-4]. An ideal controlled release systems is the form who can deliver a drug at a specified rate and keep a therapeutically effective level for the drug concentration in the organism [5]. One method to control the release of drug is the use of membranes as a release system [6]. The mechanism of the drugs released across the membrane can be the diffusivity through the membrane, according to Fick's law [7].

Among the polymers, the polyurethanes used in drug delivery are of considerable interest. They are an important class of polymers that have found many biomedical applications such as artificial blood vessel [8], controlled release devices [9], relatively good resistance in medium of free radical agents [10] and the possibility of changing their properties by varying soft and hard segments from the macromolecular chain [11,12]. Several approaches have been utilized to incorporate antimicrobial agents in the polyurethane matrix in attempts to eliminate the possibility of infections. It was utilized poly (tetramethylene glycol) diol or polyethylene glycol [13] as soft segment and 4,4'-methylene diphenyl diisocyante [14] and different diols as hard segment.

Different studies have been reported that the mechanism of diffusion for the release of antibiotics from the polyurethane matrices was dependent on their solubility and also by their loading concentration in the polymer matrix [15]. Another study shows that the release of the drug is influenced by the particle size and the dose of drugs in the polymers [16]. The drug release is controlled by the asymmetric membrane obtained *in vitro* or *in vivo* by polymer phase inversion [17]. Thus, release of drug from the polyurethane matrix can be influenced also by using "pore formers" incorporated into a polymer matrix [18]. Also, the surface morphology can influence the delivery rates of the drug and in correlation with the wettability can define the biological properties of the obtained systems [19].

Many different types of rifampicin release have been obtained to improve clinical efficacy of the drug [20,21]. Basak *et al*. studied the release profile of rifampicin from polyurethane with poly (ethylene glycol) and poly (ethylene lactate) ester diol as soft segment [19]. The release profile of rifampicin was characterized by a burst release followed by a sustained release of

*Address correspondence to this author at the "Petru Poni" Institute of Macromolecular Chemistry, 41A Grigore Ghica Voda Alley, 700487, Iasi, Romania; Tel: +40232217454; Fax: +40232211299; E-mail: vladus@icmpp.ro

E-ISSN: 2311-8717/14

antibacterial agent. The release of the rifampicin was study also from the copolymers styrene and ether methyl or ethyl methacrylate films [20]. The sets of the polymer films have the same profile of release, an initial phase with a high rate of release and then a significantly slower rate [20]. The antimicrobial spectrum of rifampicin includes important gram-positive and gram-negative pathogens. A sustained-release of rifampicin can be advantageous.

In the present work drug release from the polyurethane-rifampicin membranes with two concentrations in urethane group: 1.5mmol/g and 2.5 mmol/g were analyzed. Their structural and morphological properties, the contact angle measurements, as well as moisture sorption properties such as diffusion coefficients of the polyurethane-rifampicin membranes are studied. Finally, the antimicrobial activity of them is analyzed.

EXPERIMENTAL PART

Materials

Poly(tetramethylene oxide) (PTMO), Mn 2000 Da, (Sigma-Aldrich, UK); poly (butylene adipate) diol (PBA), Mn 2000 Da, (Sigma-Aldrich, UK); 1,4-butane diol (BD), (Sigma-Aldrich, UK) and 4,4'-methylene diphenyl diisocyanate (MDI), (Sigma-Aldrich, UK), were used as received. Dimethylformamide (DMF), (Sigma-Aldrich, UK), was dried over molecular sieve before use. Rifampicin (R) was offered by S.C. Antibiotice SA Iasi and was used as received. All other chemicals were of analytical reagent grade.

Polyurethanes Synthesis

The polyurethanes were synthesized from PTMO, PBA, BD and MDI in solution of DMF. The polyols PBA and PTMO were dehydrated at 120 °C, low pressure of 0.2 mmHg for 2 h. Then an equivalent quantity of MDI was added with DMF as solvent and BD as chain extender. The polyaddition reaction was carried out under stirring at temperature of 60 °C, for 4 h. The reaction of polymerization was stopped with 10 mL solution of 5 mL ethyl alcohol and 5 mL DMF, at a viscosity of 7000 cP for PU_1 and 7200 cP for PU_2, respectively at 20 °C.

Preparation of Polyurethane-Rifampicin Solutions

Initially, we have made a solution of 45 mg of rifampicin in 1.5 mL of DMF. After complete dissolution of drug, the rifampicin solution was added to 5 g polyurethane solution then was stirred vigorously for 3 h and poured on Petri-dishes (Ø=110mm). The solution obtained was left in Petri for 24 h. In the same way both types of polyurethane-rifampicin (PU-R) solutions were obtained.

Preparation of Polyurethane-Rifampicin Membranes

Polyurethane-rifampicin solutions were processed as membranes by using the phase inversion method initiated by precipitation in non-solvent [22]. The immersion of polyurethane solution obtained previously in nonsolvent bath make the solvent (DMF) - nonsolvent (MilliQ water) exchange. The deionized water at 45 °C was poured over polyurethane-rifampicin solution and kept under these conditions until the membrane separated completely from the Petri dish. Then the membranes were dried in vacuum oven 25 °C and 0.2 mbar to a constant weight. The percentage of rifampicin remained in the membranes is lower than the initial amount of rifampicin introduced due to phase inversion process. We have calculated the release of rifampicin in distilled water using the slope and the intercept obtained from the standard curve of rifampicin, in distilled water. After this the proportions of rifampicin remained in the membranes, were of 2.2% (w/w) for PU_1-R and 2.6% (w/w) for PU_2-R, respectively.

Measurements

UV-VIS Absorption Spectroscopy

The UV-VIS determinations were performed with a JENWAY type 6505 spectrophotometer (Bibby Scientific Ltd., England).

FTIR Spectra

The membranes were recorded by ATR method by means of a FT-IR DIGILAB, a Scimitar Series (USA) spectrometer with a resolution of 4 cm^{-1}. A crystal from SeZn with refraction index of 2.4 was used. The spectra were recorded over 600–4000 cm^{-1} domain at room temperature and a resolution of 4 cm^{-1}. The penetration degree was in the range of about 2–3 μm.

Differential Scanning Calorimetry (DSC)

DSC measurements were performed by means of a Pyris Diamond (Perkin Elmer) instrument. The samples mass of 6–8 mg were placed in aluminum foil pans. DSC curves were recorded in nitrogen atmosphere (20 mL/min flow) with a heating rate of 5 °C/min from -100 to -40 °C temperature range. The inflexion point of DSC curve was taken as glass transition temperature (Tg). Two runs were performed for each sample. As reference, was used high purity (98%) indium, which

has melting temperature at 156.68 °C and melting enthalpy of 28.4 J/g.

Dynamic Vapour Sorption (DVS)

The experiments was made with a fully automated gravimetric analyzer IGAsorp supplied by Hiden Analytical, Warrington (UK). The ultra-sensitive microbalance has a 0.1 µg resolution for 100 mg range and a 200 mg capacity. Level of humidity is controlled to desired RH set-point by mixing wet and dry gas (N2) streams. The measurement range of relative humidity is between 1% RH and 95% RH with an accuracy of +/- 1% (0-90 % RH) and +/-2% (90-95 % RH). The measurement range of temperature is between 5 and 80 ^{o}C with an accuracy of +/-0.05 ^{o}C. The sample container is a gas permeable micromesh stainless pan for solids. The samples were dried at 25 ^{o}C under flowing nitrogen until the weight of each sample is in equilibrium at RH<1%. The obtained value is considered the dry mass. After drying, the absorption curve is determined. After the maximum level for RH has been reached, desorption steps can be obtained.

Surface Morphology

SEM analysis was performed by employing a Vega Tescan SBH microscope using secondary electrons as signal. The microscope is entirely operated by computer and contains an electron gun with tungsten filament at an acceleration voltage of 30 KV. Images of surfaces and cross-sections were taken from the most relevant aspects. For statistical analysis the software Image J version 1.43u (available from the National Institute of Health, USA) was used from the center of each image (a square of 100 µm^2) to obtained the average size of pores and their distributions.

Contact Angle Measurements

The measurements of the contact angle were done with a KSVCAM 101 goniometry. The static drop technique was used at room temperature. The system has a CCD camera connected to a computer, which is analysed the contact angle (five measurements for each surface). A drop of liquid (~1 µL) was placed on the surface of the membrane and the image was captured with the CCD camera of the computer for analysis. The measurements have the same temperature and moisture during the experiment (23 °C and 70% respectively).

AFM Study

The measurements of the atomic force microscopy (AFM) were made in the tapping mode with a Scanning Probe Microscope (Solver PRO-M, NTMDT, Russia) and commercially available NSG10/Au Silicon cantilevers. The manufacturer's values for the probe tip radius are 10 nm, and the typical force constants are 11.5 N/m. The roughness factor was calculated as the ratio of real surface area and the geometric surface of the polyurethane membranes with SPIP4.8.4 software [23]. The three-dimensional image analysis of the surface properties using the surface roughness parameter was obtained.

In Vitro Drug Delivery

The drug release kinetics of the polyurethane-rifampicin membrane was carried out as follows. The experiments were performing in a shaking bath thermostated at 37 °C by immersing 10 mm^2 squared shaped samples (about 0.02 g) of the amounts of polyurethanes-rifampicin membranes in 15 mL sealed glass vial of the phosphate buffer (PB) (pH 7.4, 0.01M). The release was made by changing the phosphate buffer at 24 h and at certain time intervals aliquots (1 mL) of the sample were withdrawn periodically to determine drug concentration. The released of rifampicin amount was monitored using a UV-VIS Spectrophotometer Varian Cary-100 BIO. The absorbance of rifampicin was determined at a wavelength of 475 nm [1]. The amount of rifampicin released from the membranes, at a given time, was calculated using the slope and the intercept obtained from the standard curve of rifampicin in phosphate buffer pH=7.4, prepared for pure drug in the appropriate concentration region. Experiments were performed in duplicate, and the average value was considered.

Mechanism of Release

For analysed the release data the Korsmeyer–Peppas equation was used. The release rate k and the diffusion coefficient n of each membrane-rifampicin were calculated by linear regression analysis.

$$M_t / M_\infty = k \cdot t^n \tag{6}$$

where: M_t/M_∞ is the of drug release rapport at a predefined time t, k is a constant who contain the structural and geometric characteristics of the sustained release system and n, the release exponent, a parameter used to characterise the mechanism of diffusion [24].

Antibacterial Activity

The antibacterial activity of the polyurethane membranes with rifampicin was assessed *in vitro* by a modified Kirby-Bauer test [13]. The activity was tested

against a gram positive *S. Epidermidis* RP 62A, a gram negative *P. Aeruginosa* ATCC 1544. Mueller–Hinton milieu was used throughout the test. Sterile molten Mueller–Hinton agar was poured into sterile disposable Petri dishes (Ø: 100 mm). Cultures were prepared in a sterile Mueller–Hinton broth and were vortexed for 24 h at 37 °C. The bacterial suspensions (10^7 CFU/mL) were transferred individually onto the surface of Mueller-Hinton agar plates. The disks with 18 mm of PU membrane were placed in these Petri plates. After incubation at 37 °C for 24 h, the inhibition zone of the bacterial growth around the rifampicin polyurethane membrane was measured from one edge of the zone of inhibition to the opposite edge, including the diameter of the disk. After that measure, all disks were transferred to new seeded Petri plates. The colony forming unit (CFU/mL) of each dilution was determined after a serial dilution and count for colonies on Mueller–Hinton agar. The rifampicin diffuses out and inhibits the growth of bacteria resulting in a zone of inhibition.

RESULTS AND DISCUSSION

The polyurethanes were synthesized from PTMO, PBA, BD and MDI in solution of DMF according to previously published method [2, 12]. Briefly, the polyurethane PU_1 was synthesized with the molar components ratio PTMO: PBA: MDI: BD of 1:1:3.8:1.8 and the polyurethane PU_2 in the ratio PTMO: PBA: MDI: BD of 1:1:8.4:6.4. The synthesis of the polyurethanes PU_1 and PU_2 are presented in Scheme **1**.

ATR-FTIR Analysis

The representative ATR–FTIR absorbance bands observed in the spectra of PU_1 and PU_2 and their membranes polyurethanes-rifampicin are presented in Figure **1**. The spectrum of PU_1 and PU_2 displays a broad intense absorption bands with the maximum at 3335, 3330 cm^{-1} respectively; assigned to ν(N-H) stretching bounding [12], and the peaks at 2943, 2942 cm^{-1} respectively, are the asymmetric and symmetric stretching vibration $\nu(CH_2)$ of the soft segment [12]. The both free carbonyl groups of polyester chain and urethane groups ν(C=O) are at 1729, 1728 cm^{-1} and the stretching vibrations of bonding carbonyl groups ν(C=O) of urethane structure is at 1712, 1701 cm^{-1} respectively [2-4, 12]. Also the ATR-FTIR displays a broad intense absorption bands with the maximum at 1596, 1597 cm^{-1}, respectively for the stretching vibration ν(C=C) of aromatic ring; the peaks at the 1529, 1532 cm^{-1}, amide II consist mainly from the deformation vibrations δ (N-H) and stretching vibrations ν(C-N) and at the 1220 and 1221cm^{-1} the amide III is at the same type of vibrations δ(N-H) and ν(C-N) respectively [12, 25].

The characteristic peaks of rifampicin were identified at 3439 cm^{-1} for the stretching vibration of hydrogen free; the 2970 and 2917 cm^{-1} for the asymmetric and symmetric stretching vibration $\nu(CH_2)_{asy}$, $\nu(CH_2)_{sym}$ and the 1734, 1710 cm^{-1} for the stretching vibration of free and bonding carbonyl ν(C=O) [21]. The intensive peak of the stretching vibration ν(C=C) is at 1565 cm^{-1} and the peak of stretching vibration ν(C-O-C) is at 1020 cm^{-1} [21]. We note that was used Form II of rifampicin which have 2 peaks in the carbonyl region at 1714 and 1734 cm^{-1}, the typically found crystalline form of the drug [21].

The Table **1** shows the assignments of the major ATR-FTIR absorption bands in the polyurethane membranes, which demonstrate the presence of the expected functional groups. This bands overlap with

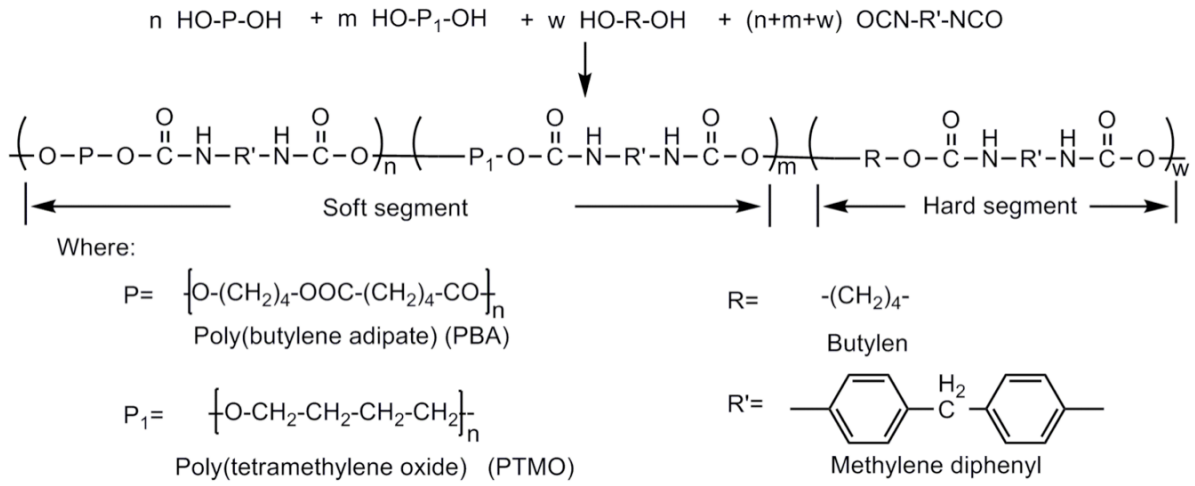

Scheme 1: Synthesis of the polyurethane samples.

Table 1: Assignment of the Major ATR-FTIR Absorption Bands

Assignment	Intensity*	Wavenumbers, (cm^{-1})	
		PU_1/PU_1R	***PU_2/PU_2R***
ν(N-H), hydrogen-bonded	w, m	3335/3336	3330/3331
ν $(CH_2)_{asym}$	m	2943/2942	2943/2942
ν $(CH_2)_{sym}$	m	2861/2862	2858/2862
ν(C=O), urethane carbonyl free	vs	1728/1728	1729/1728
ν(C=O), hydrogen bonded urethane carbonyl	vs	1704/1702	1701/1701
ν(C=C) aromatic ring	m	1597/1597	1596/1597
δ(N-H)+ ν(C-N), amide II	s	1532/1532	1529/1532
δ (C-H) scissoring and bending	w	1414/1413	1413/1413
δ(N-H) + ν (C-N), amide III	vs	1220/1220	1221/1220
ν(C-O) in ether group	s	1170/1171	1106/1107
ν$(C\text{-}O\text{-}C)_{sym}$, aliphatic ether and ester group	vs	1107/1106	1078/1078
CH_2 rocking vibration	w	771/771.3	771/771.3

*w, weak; m, medium; s, strong; vs, very strong.

the absorption bands of rifampicin, which have the same type of groups and vibrate at the same wavelength.

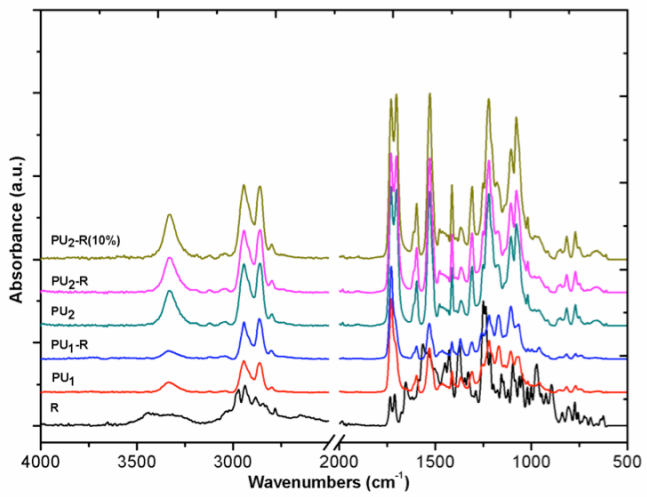

Figure 1: ATR-FTIR spectra of PU_1, PU_2, PU_1-R, PU_2-R, PU_2-R (10%) and R.

At the spectra PU_1, PU_2, PU_1-R and PU_2-R are not major differences among them, probably for the less concentration of rifampicin. The different intensity of the stretching bounding ν(N-H) between PU_1 and PU_2 is influenced by the amount of hard segment. The analysis of the carbonyl absorption region in the polyurethane spectra can provide information related to the formation of the hydrogen bonds [26]. The changes of the polyurethane structure with rifampicin can be better highlight at the carbonyl band, for the concentration of 10% w/w rifampicin in the region 1800 – 1650 cm^{-1}.

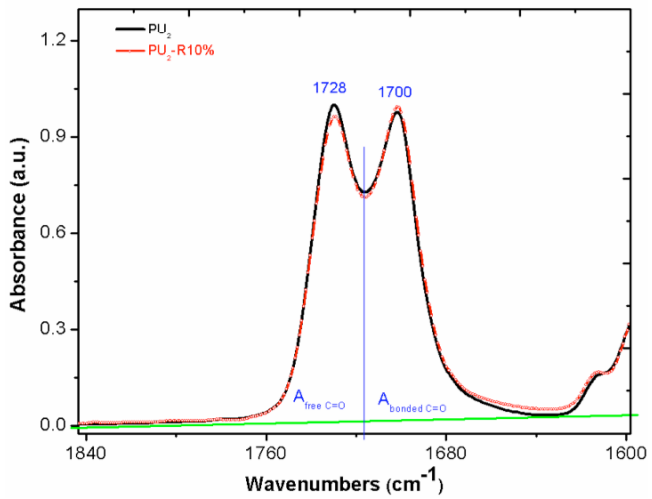

Figure 2: The carbonyl bands in region 1800-1630cm^{-1}: black - PU_2 and red-PU_2 with10% R.

The absorbance of the carbonyl bond peak PU_2 from 1700 cm^{-1} increased at the concentration 10% rifampicin. The free hydrogen of rifampicin was interacting with the free carbonyl of urethane from 1728 cm^{-1} and formed hydrogen bonds (Figure **2**). In the carbonyl region 1800-1630 cm^{-1} the ratio between the area of the absorption band of free carbonyl and the area of the absorption band of bonded carbonyl is in the relation ($A_{freeC=O:}A_{bond\ C=O}$) 1:1.06 for PU_2 and 1:1.14 for PU_2-10R, respectively.

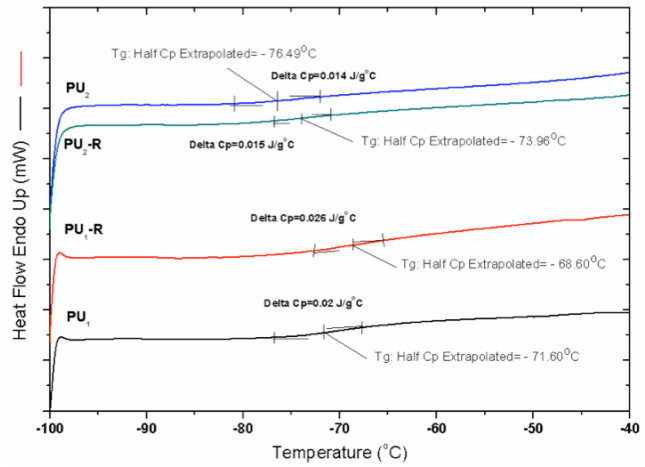

Figure 3: DSC curves of PU_1 and PU_2 and the PU_1-R and PU_2-R.

DSC Analysis

The DSC curves of PU_1, PU_2 respectively, with rifampicin and the values of glass transition temperature (T_g) are presented in the Figure **3**. The glass transition temperature of PU_2 is lower by comparison to PU_2 due to the crystalline-amorphous phase separation that is specific to polyurethanes, when the concentration in urethane groups it is more than 2 mmol/g [2-4, 12]. The incorporation of the rifampicin into the polyurethane matrix increased the values of the glass transition temperature of the amorphous phase of polyurethane [27]. The phenomenon may be attributed to the interactions between rifampicin and polyurethanes and is in accordance with the ability of rifampicin to form hydrogen bonds, reported also by other polymers system [27, 28].

Water Sorption/Desorption Isotherms

Dynamic Vapor Sorption is an important instrument that can evaluate the effects on surface absorption moisture. Water vapors sorption capacity for the samples at 37 °C in the 0-90% relative humidity range (RH) was investigated by using the IGAsorp equipment. The vapors pressure was increased in 10% humidity steps, every having a pre-established equilibrium time between 10-20 minutes. Drying sample before sorption measurements was carried out at 37 °C in flowing nitrogen (250 mL/min) until the

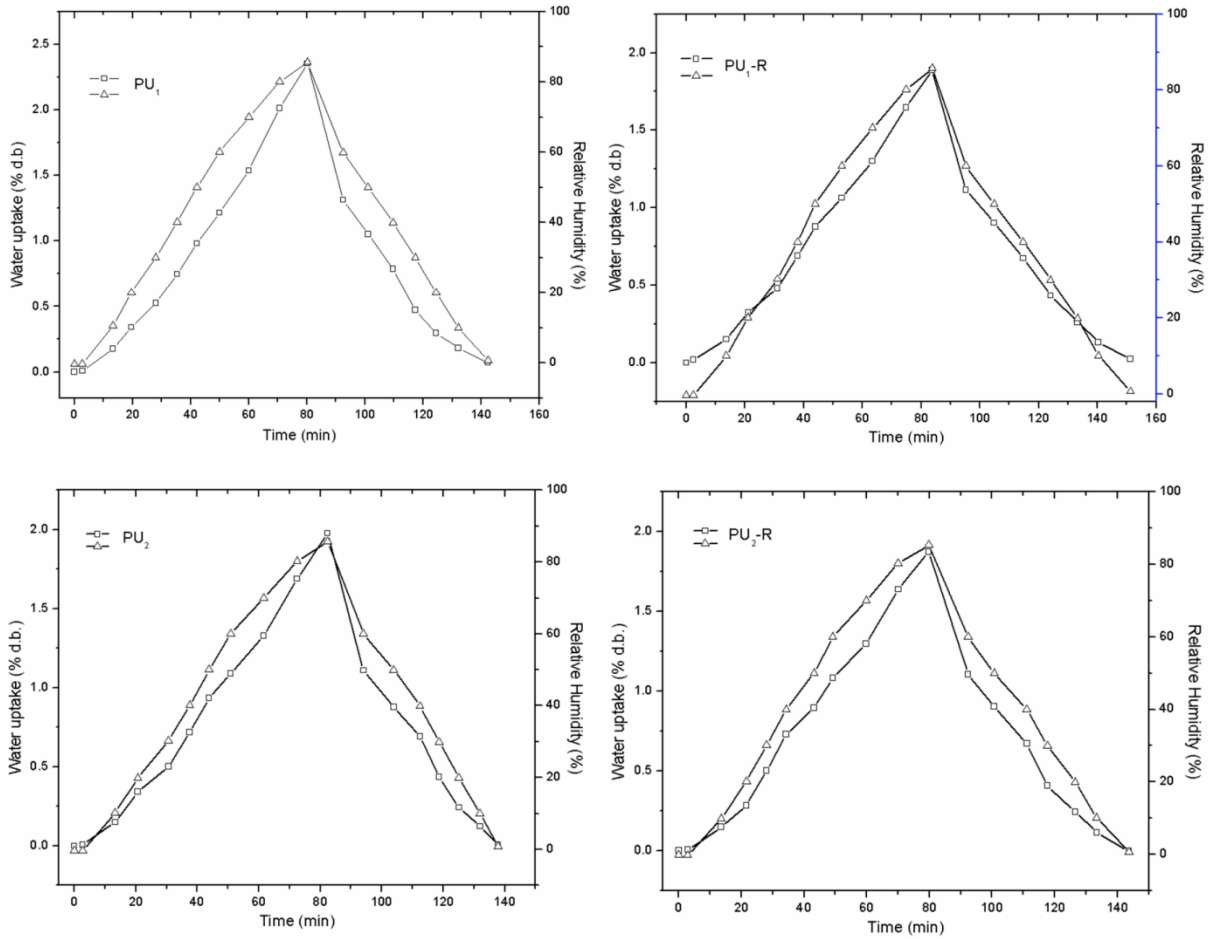

Figure 4: Water-uptake (□) and Relative Humidity (Δ) versus Time during dynamic vapor sorption test.

weight of the sample was in equilibrium at RH<1%. The sorption/desorption isotherms registered in these conditions are presented in Figure **4**.

From Figure **4** is presented the sorption-desorption behavior of the membranes studied. The obtained results are probably due to several differences between sorption and desorption process from the polymer structure rearrangement and also to the differences in the initial and final morphological states of the two processes.

Diffusion Coefficients

In the polymer materials, moisture diffusion [29, 30] is a very complex process. Diffusion coefficients can be determined from kinetic sorption data. The samples used in this study are relatively thin (l<0.5 mm). The diffusion from the edges of the film is neglected, only a concentration gradient along the x-axis exists. Based on Fick's first and second law, Crank [31] deduced that in these cases the diffusion coefficient at short time scales (M_t/M_∞ <0.5) can be described by:

$$\frac{M_t}{M_\infty} = \frac{4}{l} \cdot \sqrt{\frac{D \cdot t}{\pi}} \quad (1)$$

where M_t [g] is the mass of sorbed water vapor at time t [s], M_∞ [g] is the mass sorbed at t = ∞, l [cm] is the polymer film thickness and D [cm^2/s] is the Fickian diffusion coefficient.

The Fickian diffusion coefficient for water in the polymer matrix can thus be determined from the initial slope of a plot of M_t/M_∞ versus $t^{1/2}$ (as can be extracted from kinetic sorption experiments).

At longer time scales (M_t/M_∞>0.5) the Fickian diffusion coefficient can be calculated from:

$$\frac{M_t}{M_\infty} = 1 - \frac{8}{\pi^2} \cdot e^{-\frac{D\pi^2 t}{l^2}} \quad (2)$$

where M_t [g] is the mass of water vapor absorbed at time t [s], M_∞ [g] is the mass penetrated at t = ∞, l [cm] is the polymer film thickness and D [cm^2/s] is the Fickian diffusion coefficient. In this case the Fickian diffusion coefficient can be deduced from the slope of a plot of $ln(1-M_t/M_\infty)$ vs. t.

From the Figure **5**, the diffusions coefficients were determined. The Table **2** show the values of the diffusion coefficients, using Eq. (1) and Eq. (2), respectively.

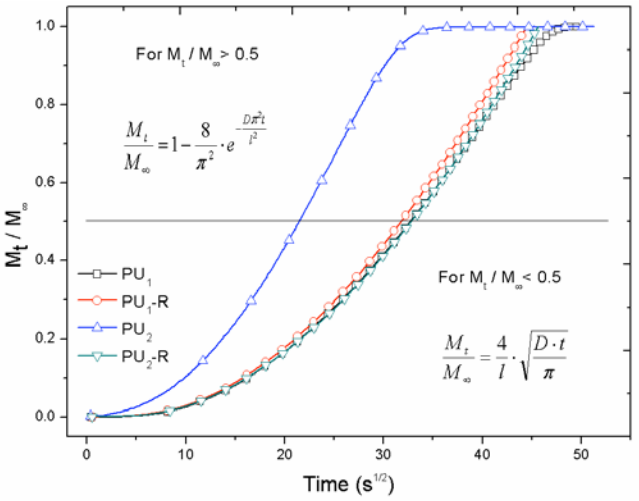

Figure 5: Graphical representation of normalized mass changing vs. time ½ of PU_1, PU_2, PU_1-R and PU_2-R.

Table 2: Parameters and Coefficients Diffusion of PU_1, PU_2 and PU_1-R, PU_2-R Respectively

Sample	M_t/M_∞<0.5	M_t/M_∞>0.5	l (cm)
	D_1 (cm^2/s)	D_2 (cm^2/s)	
PU_1	$1.11 \cdot 10^{-7}$	$6.52 \cdot 10^{-7}$	0.045
PU_1-R	$1.17 \cdot 10^{-7}$	$7.59 \cdot 10^{-7}$	0.045
PU_2	$8.51 \cdot 10^{-8}$	$5.79 \cdot 10^{-7}$	0.045
PU_2-R	$1.10 \cdot 10^{-7}$	$7.32 \cdot 10^{-7}$	0.045

The results obtained from the Table **2** estimated the values of the diffusion coefficients disposed in the following order: PU_1-R >PU_1 >PU_2-R>PU_2. The obtained values for the polyurethane PU_1-R, PU_2-R increased slowly due to the morphology of the membranes and pore size distribution for polyurethane with rifampicin as revealed by AFM photos and SEM micrographs.

Contact Angle and Surface Free Energy

The hydrophobic or hydrophilic properties of the polymer surface are important for establishing the biocompatibility of the polymeric materials [32]. Solid surface dynamics can be described by contact angle measurements. The contact angle represents the interactions of the three interfaces as described by Young's equation:

$$\gamma_{LV} \cos\theta = \gamma_{SV} - \gamma_{SL} \quad (3)$$

where γ_{SV} is the energy of the surface, γ_{SL} is the interfacial tension between the solid and the drop, γ_{LV}

is the liquid-vapour surface tension, and cos θ is the contact angle of the drop with the surface [33].

The measured contact angles of polyurethane membranes and polyurethane rifampicin membranes are given in Table **3**. The water contact angle for PU_1 (98^o) has a value much lower than PU_2 (122^o). These variations can be ascribed to the modification of the surface chemistry of the polyurethanes. It is well known that any increase in crystallinity of polymer ultimately results in increasing the hydrophobic character of the polymers [34]. The rifampicin is considered a hydrophilic drug, soluble in pH 7.4 phosphate buffer [35]. However, the Table **3** depicted that the value of contact angle obtained decreased very slow with the addition of the rifampicin probably for his concentrations in polyurethanes-rifampicin membranes. The surface free energy (γ_{SV}) was determined from the contact angle measurements. It can be divided into two components: polar component (γ^p_{SV}) including two types of Coulomb interactions dipole-dipole and dipole-induced dipole, and dispersive component (γ^d_{SV},) represented the van der Waals interactions [36]. The values of the surface-free energy (γ_{SV}) as well as the polar (γ^p_{SV}) and dispersive (γ^d_{SV}) components were obtained according to the Owens-Wendt-Rabel, and Kaelbe method [33]:

$$\gamma_{SV} = \gamma^p_{SV} + \gamma^d_{SV} \quad (4)$$

$$W_a = 2\left(\sqrt{\gamma^d_{SV}\gamma^d_{LV}} + \sqrt{\gamma^p_{SV}\gamma^p_{LV}}\right) \quad (5)$$

where W_a is the work of adhesion.

The work of adhesion (W_a), the dispersive component (γ^d_{SV},) and the polar component (γ^p_{SV}) of the surface tension (γ_{SV}) are given in Table **3**. It is clear from our results that both the work adhesion and the polar components decreased while the dispersive component increased with the amount of the urethane concentration in PU_2. The dispersive and polar surface tension parameters evaluated are strongly influenced by composition of the polyurethane-drug membrane. Furthermore if the contact angle decreases it implies that the wetting of the surface is better. Also, the water might wet the surface to higher extent, with a higher rate of the rifampicin release [21]. Seen from the perspective of the contact angles, the behaviour of the release for the two polyurethane PU_1 and PU_2 with rifampicin is a more sustained release of PU_2 compared with PU_1.

Morphological Analyses of Membranes

The surface section of the rifampicin membrane taken before and after drug release studies is presented in Figure **6**. The mechanism of the water penetration through the microporous membranes is complex in addition to a simple transport of water molecules through micro-capillaries [1]. The membranes polyurethane with rifampicin has interconnected pores, non-individual circular shape pores with various sizes. For statistical analysis, image processing software ImageJ (NIH, USA) was used to measure the pore diameters from SEM micrographs. In the diagram distribution of the pores, the analyzed polyurethane membranes before and after released of rifampicin (Figure **6**), show no major change in the size of pore distributions after the completed dissolution study. Due to the large pores, the mechanism governing diffusion phenomena may be Fickian diffusion, and the zero-order release rate will not be achieved [37]. The main interest was to see how the morphology of the polyurethane with rifampicin influences the release of drug. We conclude that the antibiotic release is influence also by the surface phenomenon because was observed that a rougher surface constitutes a larger area for release.

Atomic Force Microscopy

The atomic force microscopy (AFM) images present the topographical and morphological features of the PU_1, PU_2, PU_1-R and PU_2-R surface (Figure **7**). The three-dimensional topographies obtained by AFM for the polyurethane with rifampicin exhibit different

Table 3: Water Contact Angle, Work of Adhesion, Surface Free Energy and Polar and Dispersive Components of the Surface Free Energy Measurements

Sample	θ (°	W_a mN/m	γ_{SV} mN/m	γ^p_{SV} mN/m	γ^d_{SV} mN/m
PU_1	98.00±0.28	62.66	21.83	2.226	19.61
PU_2	112.02±0.76	45.52	28.81	0.100	28.71
PU_1-R	90.00±0.98	72.80	31.93	2.38	29.55
PU_2-R	104.86±0.92	54.13	43.02	0.237	42.78

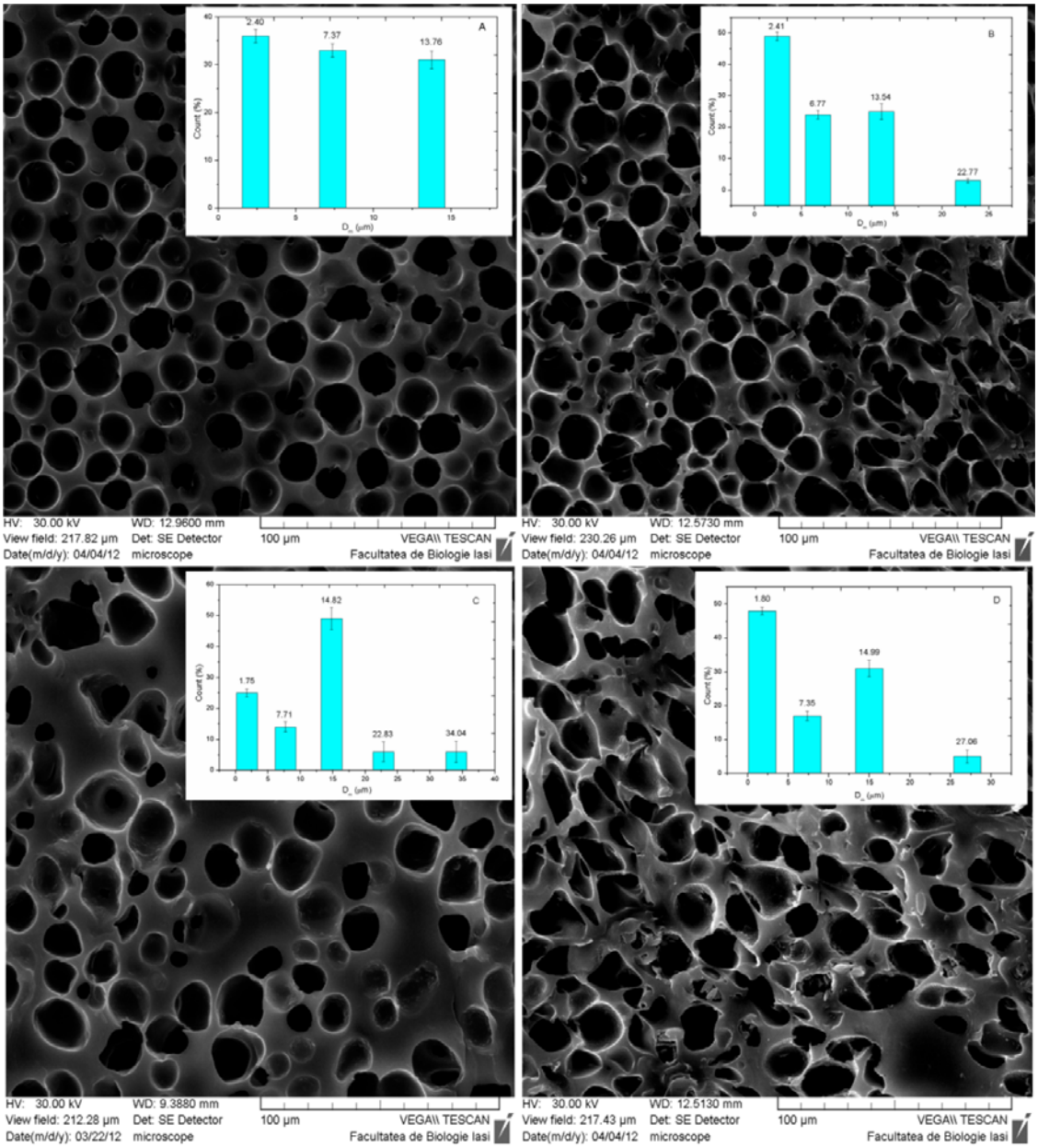

Figure 6: SEM (x100) of cross-section: A) PU_1-R before release (D_m-7.56 µm); B) PU_1-R after release (D_m-6.85 µm); C) PU_2-R before release (D_m-11.52 µm); D) PU_2-R after release (D_m-8.29 µm).

changes in the surface morphology, indicating the possibility of interaction between the urethane groups and rifampicin. Thus the factors of roughness (FR) are for PU_1-R of 1.0366 and for PU_2-R of 1.00781 respectively, indicating a smoother surface of PU_2-R than the surface of the PU_1-R. This can be understood simply by the fact that a rougher surface constitutes a larger area for release. This thing supports the idea that the antibiotic release is influence also by the surface phenomenon [38].

In Vitro Release Study

In our work, the release behaviour of rifampicin from polyurethane membranes was studied by immersing polymeric samples into phosphate buffered (pH=7.4) at 37 °C (Figure **8**). Similarly drug release profile of both formulations membrane PU_1-R and PU_2-R exhibits an initial burst release and then a sustained release of rifampicin through polyurethane membranes. The release profile depicts that rifampicin release is highly influenced by the concentration of urethane groups but also by the surface of polymers: as the urethane concentrations increased the release of rifampicin decreased.

The linear regression analysis for the release experiments of rifampicin measured in the interval 48-216 h reported that the PU_1-R released 0.0142 µg/mL

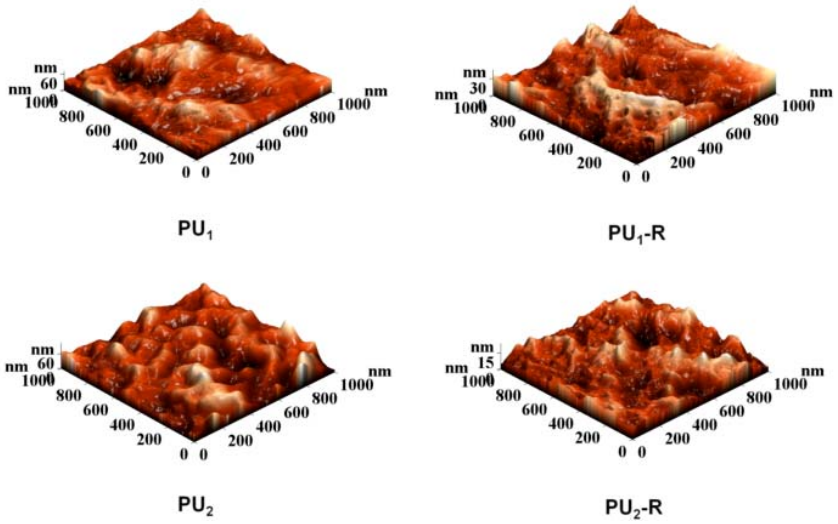

Figure 7: AFM 3D image of PU_1, PU_2, PU_1-R and PU_2-R.

while the PU_2-R released only 0.0121 µg/mL. This indicates a prolonged release of rifampicin from polyurethane matrix PU_2-R. The obtained release values are much higher than the minimum inhibitory concentration (MIC) of rifampicin for Gram-positive bacteria [39, 40]. The effect of a sustained release for the concentration in urethane 2.5 mmol/g was observed also at the release of nystatin from these polyurethanes [2].

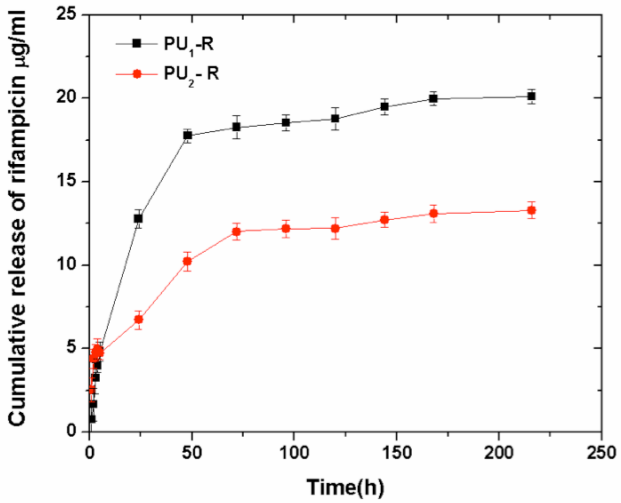

Figure 8: Cumulative release of rifampicin vs. time from PU_1-R and PU_2-R membranes.

Mechanism of Drug Release

The diffusion process occurs when a drug or other active agent passes through the polymer, at the macroscopic scale (through pores in the polymer matrix) and at the molecular level (by passing between polymer chains) [41]. The 'n' and 'r' squared values are given in Table **4**, where the values of 'n' were 0.5431 for PU_1-R and 0.5301 for PU_2-R, respectively. By observing the value of 'n' for Korsmeyer–Peppas relationship, it appears that the mechanism of diffusion is the Fickian one. The same mechanism of Fickian diffusion was obtained also in the case of the release of nystatin from these polyurethanes matrix [2]. We can assume an overall release of minimum 10 days (Figure **8**).

Table 4: Values of *r* and *n* Coefficients from Korsemeyer-Peppas Relation

Sample	*n*	r^2
PU_1-R	0.5431	0.9517
PU_2-R	0.5301	0.9631

Antibacterial Activity

The release of rifampicin polyurethane membranes in the first hour is greater than the minimum inhibitory concentration against the Gram-positive bacteria (lower than 0.006 µg/mL for *S. Aureus* [37] <0.016 µg/mL for *S. Epidermidis* RP 62 A) [40]. The antibacterial activity of the polyurethane rifampicin membrane against *S. Epidermidis* RP 62 A and *P. Aeruginosa* ATCC 1544 is determined (Figure **9**). All membranes with rifampicin produced a diameter of the inhibition zone when placed in plates overlaid with *S. Epidermidis* and *P. Aeruginosa*, while the control polymer membrane without rifampicin showed no inhibition zone. The effect was maintained during a prolonged period by a low rifampicin amount released sufficiently active in the case of *S. Epidermidis*. The species of *P. Aeruginosa* are intrinsically resistant to rifampicin [42].

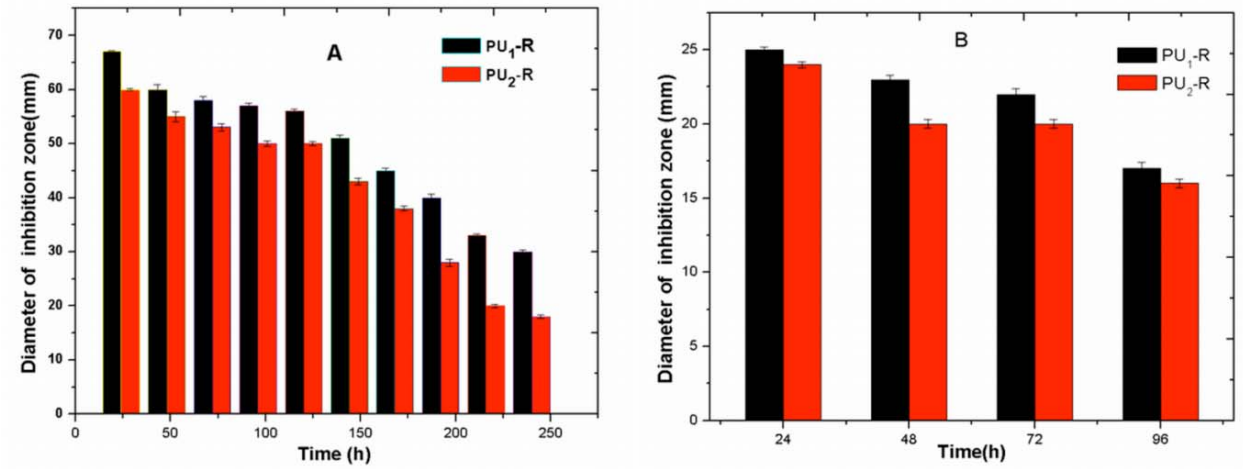

Figure 9: Diameter of the inhibition zone for PU_1-R and PU_2-R against **A**) *S. Epidermidis* and **B**) *P. Aeruginosa.*

However, the release of rifampicin is in correlation with the diameter of inhibition zone, for PU_1-R is relatively greater than that of PU_2-R in both bacterial studies (Figure **9**). Despite the good activity against the *S. Epidermidis* the rifampicin polyurethane membrane was able to suppress the bacterial colonization rate but did not kill all the microorganisms during the testing.

CONCLUSIONS

Polyurethane based on two concentrations in urethane groups 1.5 $mmol.g^{-1}$ and 2.5 $mmol.g^{-1}$ was found to be used as matrix for drug delivery. It was shown that the kinetics and release mechanism depend on the morphology and structural composition of the polymer-drug membrane, who shows that the drug structure the polyurethane matrix. The release mechanism was a Fickian one, confirmed by the results from our experiments of release and SEM micrographs. The prolonged nature of the release of rifampicin is assured by the concentrations in urethane groups and also by the surface properties. The results from the release study, and the good biological activity suggests us the possibility of using these polyurethane materials in the field of biomedicine.

ACKNOWLEDGEMENT

This work was realized with the financial support of EURODOC (ID 59410), “Doctoral Scholarships for research performance at European level” project financed by the European Social Found and Romanian Government”, and a Seventh Framework Programme, NMP-2007-2.3-1, ″BIOactive highly porous and injectable Scaffolds controlling stem cell recruitment, proliferation and differentiation and enabling angiogenesis for Cardiovascular ENgineered Tissues″ (BIOSCENT), No. 214539/01.01.2009.

REFERENCES

[1] Rao B, Murthy K. Studies on rifampicin release from ethylcellulose coated nonpareil beads. Int J Pharmac 2002; 231(1): 97-106. http://dx.doi.org/10.1016/S0378-5173(01)00874-2

[2] Mandru M, Ciobanu C, Ignat M, Popa M, Verestiuc L, Vlad S. Sustained release of nystatin from polyurethane membranes for biomedical applications. Digest J Nanomater Biostruct 2011; 6(3): 1227-38.

[3] Mândru M, Vlad S, Ciobanu C, Lebrun L, Popa M. Polyurethane-hydroxypropyl cellulose membranes for sustained release of nystatin. Cellulose Chem Technol 2013; 47(1-2): 5-12.

[4] Mândru M, Ciobanu C, Vlad S, Butnaru M, Lebrun L, Popa M. Characteristics of polyurethane-based sustained release membranes for drug delivery. Cent Eur J Chem 2013; 11(4): 542-553. http://dx.doi.org/10.2478/s11532-012-0187-y

[5] Krusic M, Ilic M, Filipovic J. Swelling behaviour and paracetamol release from poly(N-isopropylacrylamide-itaconic acid) hydrogels. Polym Bull 2009; 63(2): 197-211. http://dx.doi.org/10.1007/s00289-009-0086-3

[6] Zhan X, Chen S, Tang G, Mao Z. A new copolymer membrane cured by 2-hydroxy-3-phenoxypropylacrylate, 4-hydroxybutyl acrylate, and isobutyl methacrylate controlled clonidine linear release in the transdermal drug delivery system. Polymr Adv Technol 2007; 18(5): 392-6. http://dx.doi.org/10.1002/pat.901

[7] Cardea S, Sessa M, Reverchon E. Supercritical phase inversion to form drug-loaded poly(vinylidene fluoride-co-hexafluoropropylene) membranes. Indus Eng Chem Res 2010; 49(6): 2783-9. http://dx.doi.org/10.1021/ie901616n

[8] Pennings A, Knol K, Hoppen J, Leenslag J, van der Lei B. A two-ply artificial blood vessel of polyurethane and poly(L-lactide). Coll Polym Sci 1990; 268: 2-11. http://dx.doi.org/10.1007/BF01410416

[9] Jabbari E, Khakpour M. Morphology of and release behavior from porous polyurethane microspheres. Biomaterials 2000; 21(20): 2073-9. http://dx.doi.org/10.1016/S0142-9612(00)00135-6

[10] Oprea S, Vlad S. Evaluation of physico-mechanical properties of precipitated polyurethane films in medium of free radical agents. Eur Polym J 2002; 38(7): 1465-70. http://dx.doi.org/10.1016/S0014-3057(02)00003-4

[11] Vlad S. Influence of the hard segment contents on mechanical behavior of some poly(ether-urethane-urea)s. Mater Plast 2005; 42(1): 63-7.

[12] Ciobanu C, Han X, Cascaval C, Guo F, Rosu D, Ignat L, *et al*. Influence of urethane group on properties of crosslinked polyurethane elastomers. J Appl Polym Sci 2003; 87(11): 1858-67. http://dx.doi.org/10.1002/app.11509

[13] Ruggeri V, Francolini I, Donelli G, Piozzi A. Synthesis, characterization, and *in vitro* activity of antibiotic releasing polyurethanes to prevent bacterial resistance. J Biomed Mater Res Part A 2007; 81A(2): 287-98. http://dx.doi.org/10.1002/jbm.a.30984

[14] Vlad S, Oprea S. Effect of polyols on the physico-mechanical properties of some polyurethanes. J Optoelectr Adv Mater 2007; 9(4): 994-9.

[15] Schierholz J, Steinhauser H, Rump A, Berkels R, Pulverer G. Controlled release of antibiotics from biomedical polyurethanes: Morphological and structural features. Biomaterials 1997; 18(12): 839-44. http://dx.doi.org/10.1016/S0142-9612(96)00199-8

[16] Sung K, Han R, Hu O, Hsu L, Controlled release of nalbuphine prodrugs from biodegradable polymeric matrices: influence of prodrug hydrophilicity and polymer composition. Int J Pharmac1998; 172: 17-25. http://dx.doi.org/10.1016/S0378-5173(98)00156-2

[17] DesNoyer J, McHugh A. The effect of Pluronic on the protein release kinetics of an injectable drug delivery system. J Controll Release 2003; 86(1): 15-24. http://dx.doi.org/10.1016/S0168-3659(02)00293-6

[18] Kim J, Kim S, Lee S, Lee C, Kim D. The effect of pore formers on the controlled release of cefadroxil from a polyurethane matrix. Int J Pharmac 2000; 201(1): 29-36. http://dx.doi.org/10.1016/S0378-5173(00)00388-4

[19] Paun I, Moldovan A, Luculescu C, Dinescu M. Biocompatible polymeric implants for controlled drug delivery produced by MAPLE. Appl Surf Sci 2011; 257(24): 10780-8. http://dx.doi.org/10.1016/j.apsusc.2011.07.097

[20] Basak P, Adhikari B, Banerjee I, Maiti T. Sustained release of antibiotic from polyurethane coated implant materials. J Mater Sci-Mater Med 2009; 20: 213-21. http://dx.doi.org/10.1007/s10856-008-3521-3

[21] Otto D, Vosloo H, Liebenberg W, de Villiers M. Development of microporous drug-releasing films cast from artificial nanosized latexes of poly(styrene-co-methyl methacrylate) or poly(styrene-co-ethyl methacrylate). Eur J Pharmac Biopharmac 2008; 69(3): 1121-34. http://dx.doi.org/10.1016/j.ejpb.2008.02.004

[22] Melnig V, Apostu M, Tura V, Ciobanu C. Optimization of polyurethane membranes - Morphology and structure studies. J Membr Sci 2005; 267(1-2): 58-67. http://dx.doi.org/10.1016/j.memsci.2005.04.054

[23] IUPAC Compedium of Chemical Terminology 2nd Edition 1997.

[24] Raval A, Parikh J, Engineer C. Dexamethasone eluting biodegradable polymeric matrix coated stent for intravascular drug delivery. Chem Eng Res Design 2010; 88(11A): 1479-84. http://dx.doi.org/10.1016/j.cherd.2010.03.007

[25] Janik H, Palys B, Petrovic Z. Multiphase-separated polyurethanes studied by micro-Raman spectroscopy. Macromol Rapid Commun 2003; 24(3): 265-8. http://dx.doi.org/10.1002/marc.200390039

[26] Senich G, MacKnight W. Fourier transform infrared thermal analysis of a segmented polyurethane. Macromolecules 1980; 13: 106-10. http://dx.doi.org/10.1021/ma60073a021

[27] Jones D, McCoy C, Andrews G. Physicochemical and drug diffusion analysis of rifampicin containing polyethylene glycol-poly(epsilon-caprolactone) networks designed for medical device applications. Chem Eng J 2011; 172(2-3): 1088-95. http://dx.doi.org/10.1016/j.cej.2011.05.024

[28] Agrawal S, Ashokraj Y, Bharatam P, Pillai O, Panchagnula R. Solid-state characterization of rifampicin samples and its biopharmaceutic relevance. Eur J Pharmac Sci 2004; 22(2-3): 127-44. http://dx.doi.org/10.1016/j.ejps.2004.02.011

[29] Stonadge P, Benham M, Ross D, Manwaring C, Harris I. The measurement of concentration dependent diffusion coefficients in the solid-solution alloys Pd-Y. Z. Phys Chem 1993; 181: S125-31. http://dx.doi.org/10.1524/zpch.1993.181.Part_1_2.125

[30] Wong E, Rajoo R. Moisture absorption and diffusion characterisation of packaging materials - advanced treatment. Microelectr Reliab 2003; 43(12): 2087-96. http://dx.doi.org/10.1016/S0026-2714(03)00378-0

[31] Crank J. The mathematics of diffusion, 2nd ed. New York: Oxford Clarendon Press 1975.

[32] Vlad S, Butnaru M, Filip D, Macocinschi D, Nistor A, Gradinaru L, *et al*. Polyetherurethane membranes modified with renewable resource as a potential candidate for biomedical applications. Digest J Nanomater Biostruct 2010; 5(4): 1089-100.

[33] Stamm M. Polymer surfaces and interfaces. Characterization, modification and applications. England: Springer 2008. http://dx.doi.org/10.1007/978-3-540-73865-7

[34] Zia K, Barikani M, Zuber M, Bhatti I, Barmar M. Surface characteristics of polyurethane elastomers based on chitin/1,4-butane diol blends. Int J Biol Macromol 2009; 44(2): 182-5. http://dx.doi.org/10.1016/j.ijbiomac.2008.12.004

[35] Park J, Lee K, Kwon I, Bae Y. PDMS-based polyurethanes with MPEG grafts: Mechanical properties, bacterial repellency, and release behavior of rifampicin. J Biomater Sci-Polym Ed 2001; 12(6): 629-45. http://dx.doi.org/10.1163/156856201316883458

[36] Alves P, Coelho J, Haack J, Rota A, Bruinink A, Gil M. Surface modification and characterization of thermoplastic polyurethane. Eur Polym J 2009; 45(5): 1412-9. http://dx.doi.org/10.1016/j.eurpolymj.2009.02.011

[37] Berg M, Zhai L, Cohen R, Rubner M. Controlled drug release from porous polyelectrolyte multilayers. Biomacromolecules 2006; 7(1): 357-64. http://dx.doi.org/10.1021/bm050174e

[38] van de Belt H, Neut D, Uges D, Schenk W, van Horn J, van der Mei H, *et al*. Surface roughness, porosity and wettability of gentamicin-loaded bone cements and their antibiotic release. Biomaterials 2000; 21(19): 1981-7. http://dx.doi.org/10.1016/S0142-9612(00)00082-X

[39] Lefebvre M, Jacqueline C, Amador G, Le Mabecque V, Miegeville A, Potel G, *et al*. Efficacy of daptomycin combined with rifampicin for the treatment of experimental meticillin-resistant Staphylococcus aureus (MRSA) acute osteomyelitis. Int J Antimicrob Agents 2010; 36(6): 542-4. http://dx.doi.org/10.1016/j.ijantimicag.2010.07.008

[40] Boelens J, Zaat S, Meeldijk J, Dankert J. Subcutaneous abscess formation around catheters induced by viable and nonviable Staphylococcus epidermidis as well as by small amounts of bacterial cell wall components. J Biomed Mater Res 2000; 50(4): 546-56. http://dx.doi.org/10.1002/(SICI)1097-4636(20000615)50:4<546::AID-JBM10>3.0.CO;2-Y

[41] McDonald P, Lyons J, Geever L, Higginbotham C. *In vitro* degradation and drug release from polymer blends based on poly(dl-lactide), poly(l-lactide-glycolide) and poly(epsilon-caprolactone). J Mater Sci 2010; 45(5): 1284-92. http://dx.doi.org/10.1007/s10853-009-4080-9

[42] Esmaeili F, Hosseini-Nasr M, Rad-Malekshahi M, Samadi N, Atyabi F, Dinarvand R. Preparation and antibacterial activity evaluation of rifampicin-loaded poly lactide-co-glycolide nanoparticles. Nanomed-Nanotechnol Biol Med 2007; 3(2): 161-7. http://dx.doi.org/10.1016/j.nano.2007.03.003

Received on 18-09-2013 Accepted on 20-09-2013 Published on 25-12-2013

DOI: http://dx.doi.org/10.12974/2311-8717.2013.01.01.5